Optimum E2 Effective Charges for the $d_{5/2}$-$s_{1/2}$-$d_{3/2}$ Model from a Survey of Experimental Electric Quadrupole Transition Strengths

B.H. Wildenthal and B.A. Brown

We have compiled a computer-stored data base of 300-plus experimentally determined electric quadrupole transition strengths for nuclei of $8 \leq N, Z \leq 20$. The foundation of the collection is the published compilation of Endt,[1] augmented by items taken from Endt and van der Leun[2] and by entries from the current literature. We are utilizing this data base, together with corresponding shell-model transition densities calculated from the Chung-Wildenthal wave functions,[3] to determine the empirically optimum values of the E2 effective charge for the "dsd" shell model.

Preliminary surveys of this sort with much smaller data bases[3,4] have suggested effective charges of $\tilde{e}_p$ = 1.35 e, $\tilde{e}_n$ = 0.35 e. The present study employs a somewhat different assumption about the sizes of the radial wave functions than did the first surveys. Rather than attempt to parameterize nuclear sizes with some A-dependent formula we have decided[5] to utilize the newly available precise rms values for the radii of stable ground states which are available from new electron scattering analyses and from new muonic atom data. We assume that the radial wave functions for the sd-shell nucleons have the harmonic oscillator functional form and adjust the oscillator parameter for a given A value to reproduce the experimental rms radius for the stable ground state of that A. This assumption, together with values for the one-body transition densities (obtained from the Chung-Wildenthal wave functions) and the effective nucleon charges (assumed A-independent) suffice to yield predictions for any sd-shell E2 transition.

We carry out least-squares fits of the theoretical E2 matrix elements to their presumed experimental counterparts in which the effective nucleon charges are treated as the parameters. The critical elements of such fits are:

1. data set choices
2. treatment of experimental errors
3. degrees of freedom

The choice of data set involves several different considerations. It is possible that there are A-dependent effects in the model-experiment relationships which would manifest themselves as different effective charges for different mass regions. This question can be simply answered by testing subsets of the data independently, A = 17-28 and A = 29-39, etc. A more subtle question about the data set is whether all data have model counterparts. We exclude the few data, principally for A = 18 and 38, which involve obvious intruder states, e.g., ^{18}O, 0_2^+, etc. This still leaves such transitions as ^{18}O $2_1^+ \rightarrow 0_1^+$ in question. These states are basically in the model space, but perhaps the E2 matrix elements are significantly contaminated by intruder components. We ultimately have to evaluate the impact of such data on the results and make an informed but arbitrary decision on what to include. Still another issue in constructing the data base involves the model for the radial wave functions. For well-bound states, the harmonic oscillator assumption should be adequate. However for states in which the last proton is loosely bound, the H-O model raises obvious questions. Again we address the issue by alternate inclusion and exclusion of the relevant items from the data base.

The treatment of experimental errors is less than straightforward because our model itself has intrinsic limitations which preclude a meaningful accuracy in prediction beyond limits which are imprecise but nonetheless certainly exceeded by a few extremely accurate measurements. To use the quoted experimental uncertainties without modification would bias the results very strongly towards fitting a very few, otherwise arbitrary, data. We deal with this by adding to the uncertainty of each datum a so-called "theoretical uncertainty". One choice for this "dampening term" is a value which produces a chi-square of 1.0, that is, the choice of a "theoretical error" equal to the rms experimental-theoretical deviation. This value is approximately 2 efm^2. As a compromise between this and no dampening, we also test the effects of a value 0.2 efm^2, which is still roughly ten times larger than the smallest experimental uncertainties.

The most restrictive parameterization with which the fit can be made is that of the conventional effective charge model. In this assumption, the relative values of the individuals T = 0 and T = 1 (or the proton and neutron) single particle matrix elements are fixed and only their overall magnitudes are varied, thereby determining the isoscalar and isovector effective charges. The restrictions of this parameterization can be successively reduced to the limit in which each single particle matrix element of the space is treated as a free parameter. The determination of the number of meaningful degrees of freedom in this problem is one of the goals of our survey.

Our first results show that the previously suggested values of e_p = 1.35, e_n = 0.35 are remarkably close to the best fits obtained from the new data base in a wide variety of fits. The type of agreement obtained between theory and experiment is shown in Fig. 1.

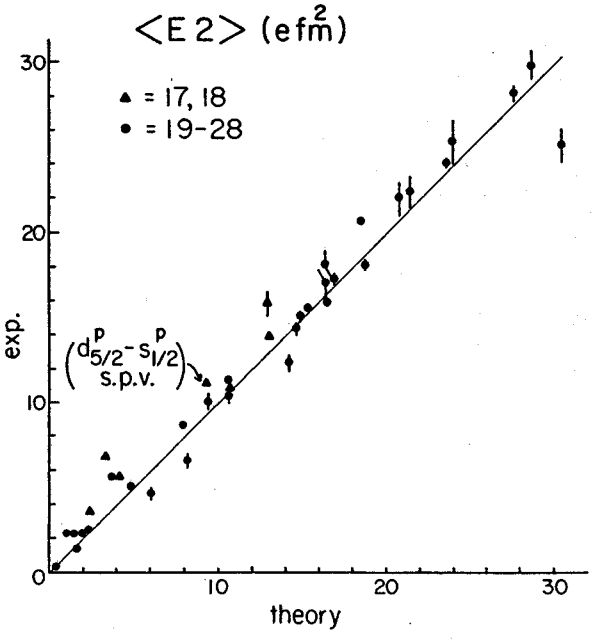

Fig. 1. Comparison of theoretical and measured matrix elements of electric quadrupole transitions. The entry for each transition is positioned such that its "x" coordinate is its theoretical value and its "y" coordinate its measured value. Perfect agreement would then correspond to a series of points all falling on the 45 diagonal. The data shown comprise those measured transitions in A = 17-28 which have assigned experimental uncertainties of less than 5%.

1. P.M. Endt, Atomic Data and Nuclear Data Tables 23 (1979) 3-61.
2. P.M. Endt and C. van der Leun, Nucl. Physics A310 (1977) 1.
3. W. Chung, Ph.D. Thesis, MSU (1976).
4. D. Schwalm, E.K. Warburton and J.W. Olness, Nucl. Phys. A293 (1977) 425-480.
5. B.A. Brown, W. Chung and B.H. Wildenthal, Phys. Rev. C22 (1980) 774.

Gamow-Teller Beta-Decay in the sd shell: A Survey of Experimental Results and the Predictions of the Chung-Wildenthal Wave Functions

B.A. Brown and B.H. Wildenthal

We have compiled the existing experimental data on allowed beta decay in the region A = 17–39 and from them extracted the matrix elements for Gamow-Teller decay. For all of these cases, as well as for decays as yet experimentally unmeasured, we have calculated from the Chung-Wildenthal wave functions (Ref. 1) for parent and daughter states the transition density matrix elements for $\Delta J = 1$, $\Delta T = 1$.

Theoretical Gamow-Teller matrix elements have been calculated from these transition densities using both the free-nucleon values for the single-particle matrix elements and the empirical values obtained in a preliminary version of this work, Ref. 2. The completion of this survey will involve a redetermination of the empirically optimum single particle matrix elements from fits to the complete data base. Inspection of the results at this stage do not suggest that the values of Ref. 2 will be changed significantly. A comparison of the predictions based on Ref. 2 to the data from the region A = 32-39 are shown in Fig. 1.

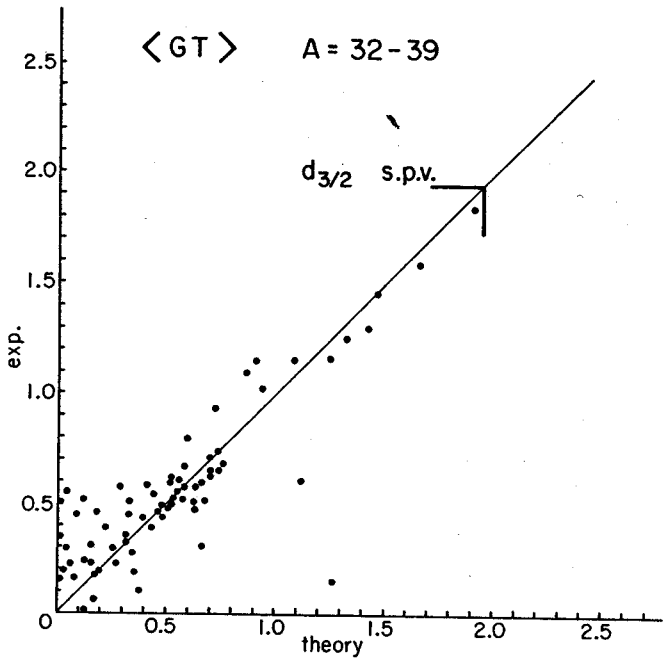

Fig. 1. Comparison between experiment and theory for the totality of Gamow-Teller beta decay matrix elements in the region A = 32-29. The theoretical values are based on the empirically renormalized single particle matrix elements.

1. W. Chung, Thesis, Michigan State University, 1976.
2. B.A. Brown, W. Chung and B.H. Wildenthal, Phys. Rev. Lett. 40, 1631 (1978).

Effects of Configuration Mixing Upon the Total Strength of $\vec{\sigma}$-like Excitation

B.H. Wildenthal and B.A. Brown

There is at present considerable activity directed towards determining if the action of the spin operator $\vec{\sigma}$ is quenched in the nucleus. Measurements of this quenching are derived from comparisons of the reduced strengths of nuclear transitions believed to be mediated by $\vec{\sigma}$ to predictions for these transitions based on models of the nuclear states involved. Hence, to be precise, we should speak of the quenching of $\vec{\sigma}$ relative to some assumed family of nuclear wave functions. It is our purpose here to demonstrate that models of different levels of reality yield similar results for some aspects of $\vec{\sigma}$ excitations and quite different results for other aspects. This "model dependence" of some types of $\vec{\sigma}$ excitation strength is suggested as the explanation for some puzzling features of magnetic dipole, and Gamow-Teller or (p,n) excitation strengths.

We direct our attention in the present investigation to the total sum of the $\vec{\sigma}$ excitation strengths from a given initial state. The elimination of concern about the details of the final state spectra allows concentration upon the ground state, the state usually best and most easily treated in a given model approximation. It also allows us to circumvent worry about the detailed matchups between individual theoretical and experimental final states. The experimental data with which these calcualtions of total strengths should be compared are, of course, those of "giant resonance" excitation studies via inelastic or charge-exchange scattering. Decay experiments, subject to inevitable Q-value limitations, very rarely sample the major portion of $\vec{\sigma}$-like strength. Hence with these latter data, comparison with theory must be on the basis of matching between individual pairs of states.

Experimental studies of the giant resonances for spin excitations of the nuclear ground state currently feature magnetic dipole electroexcitation and the (p,n) charge-exchange reactions. For now we shall assume that the angular momentum component of the transition operators for the Ml and (p,n) or β^- processes is exactly $\vec{\sigma}$. The isospin properties of these processes are, however, quite different, of course. The Ml operator leaves the projection of T, $T_z = (Z - N)/2$, unchanged and hence the isospin of the final states populated in Ml scattering must be greater than or equal to the isospin of the initial state ($T_f > (T_i = T_{z_i})$). On the other hand, the (p,n) or β^- process changes T_{z_i} to $T_{z_i} + 1$, which means that for the typical neutron-rich target, (negative T_{z_i}) the final T_z is smaller than the initial T_{z_i} in absolute magnitude and hence $T_f > |T_i - 1|$. It follows that both Ml and (p,n) or β^- excitation populate states with $T_f = T_i$ and $T_i + 1$ but that (p,n) or β^- populates, in addition, states with $T_f = T_i - 1$.

We have calculated the total strength of the excitation via the operator $\vec{\sigma}\vec{\tau}$ of the $J = 0^+$ ground states of sd nuclei using the full $d_{5/2}$ - $s_{1/2}$- $d_{3/2}$ basis-space, Chung-Wildenthal wave functions. For comparison, we have also calculated the total strengths under the assumption that, instead of the configuration - mixed C-W results, the ground state wave functions are single-component states, the wave function being the lowest (j-j) coupling basis vector in the sd-shell space. Thus, we can compare configuration-mixed to pure-configuration results in the same space. Our results are presented in Tables I and II. It is found that systematically, the strength from T = 1 to T = 0 is only slightly quenched by configuration mixing, that T = 1 to T = 1 strength is quenched by a factor of roughly two and that T = 1 to T = 2 is quenched by a factor of five to ten. The quenching which configuration mixing introduces into T = 0 to T = 1 transitions ranges between 2 to 10.

Table I. Total strength of $1.77\vec{\sigma}\vec{\tau}$ from J=0, T=1 ground states of the sd-shell to all J_f=1, T_f=0,1 and 2 states.

A(Ψ)	T_f=0	T_f=1	T_f=2
18(C-W)	17.44	1.35	
18(pure j-j)	13.78	5.01	
22(C-W)	14.74	5.11	0.21
22(pure j-j)	18.79	10.03	2.01
26(C-W)	15.15	7.86	0.84
26(pure j-j)	20.46	15.04	3.34
30(C-W)	14.96	9.22	1.08
30(pure j-j)	28.83	15.04	5.01
34(C-W)	14.01	7.65	0.57
34(pure j-j)	16.29	15.04	2.51
38(C-W)	14.87	3.93	
38(pure j-j)	11.28	7.52	

Table II. Total strengths of $1.77\vec{\sigma}\vec{\tau}$ from J=0, T=0 ground states of the sd-shell to all J_f=1, T_f=1 states.

A	20	24	28	32	36
C-W	1.39	6.16	11.39	10.14	4.19
(pure j=j)	13.37	23.39	30.08	22.56	16.04

Lifetime Predictions for ^{17}C and ^{19}N

M.S. Curtin, B.H. Wildenthal and J.A. Nolen

The completion of the k=500 superconducting heavy ion cyclotron at Michigan State University will provide intense beams in the mass 20-40 region with energies per nucleon of 20-40 MeV. This energy range is expected to be characterized by the onset of the fragmentation mechanism, a mechanism which seems particularly well suited for the production of exotic nuclei. The understanding of the nuclear structure properties of these exotic nuclei in terms of the nuclear shell model has prompted this study.

Starting with the effective Hamiltonian of Reehal and Wildenthal,[1] which spans the model space ($0p_{1/2}$, $0d_{5/2}$, $1s_{1/2}$), a level structure was generated with $j \leq 7/2$, for the nuclei ^{17}C, ^{17}N, ^{19}O, ^{19}N (see Figs. 1 and 2).

The ground state of ^{19}N was calculated to be $1/2^-$, well separated from its first excited state. However, in ^{17}C, the three lowest lying states ($5/2^+$, $3/2^+$, $1/2^+$) are all within 570 keV of each other, making it difficult to specify the J^π of the ground state. This, along with the fact that ^{15}C was observed to have an inverted ($1/2^+$) ground state directed us to consider all three possibilities as reasonable candidates for the ground state. Partial half lives associated with Gamow-Teller transitions are given according to the formula of Brown, Chung, and Wildenthal.[2]

$$ft_{1/2} = \frac{6177 \pm 14}{B(GT)_{TH}}$$

The Gamow-Teller matrix element is:

$$B(GT)^{1/2}_{TH} = \frac{1}{(2(2J_i+1))^{1/2}} \begin{pmatrix} Tf & 1 & Ti \\ -T_z f & T_z & T_{zi} \end{pmatrix} \sum_{jj'} \frac{\langle \psi f | | | (a_j^+ \times a_{j'})_\lambda | | | \psi i \rangle}{((2\Delta J+1)(2\Delta T+1))^{1/2}} \langle j | | | O_{GT} | | | j' \rangle$$

where the following values of the single particle matrix elements were used.

$$\langle d_{5/2} | | | O_{GT} | | | d_{5/2} \rangle = 8.881$$

$$\langle p_{1/2} | | | O_{GT} | | | p_{1/2} \rangle = -2.502$$

$$\langle s_{1/2} | | | O_{GT} | | | s_{1/2} \rangle = 7.506$$

The statistical factors were calculated via the prescription of Wilkinson and Macfield[5]

$$f = e^{\sum_{n=0}^{3} A_n (\ln E_o)^n} \left(\frac{1}{60}(2W_o^4 - 9W_0^2 - 8)P_o + \frac{1}{4}W_o \ln(W_o + P_o)\right)$$

W_o = total electron end point energy

$P_o = (W_0^2 - 1)^{1/2}$

The A_n's being obtained from the table in ref. 3. The Coulomb energy differences were calculated according to the formula given by de Shalit and Talmi.[4]

$$\Delta_1(z^1) = E_c(z^1+1) - E_c(z^1) = C + z^1 a + \tfrac{1}{2}(1-(-1)^{z^1})b$$

$$\Delta_2(z^1) = E_c(z^1+2) - E_c(z^1) = 2C + (2z^1+1)a + b$$

where

z^1 = # protons outside a closed shell.

Using the appropriate pairs of nuclei in the $0p_{1/2}$ shell and binding energies taken from Wapstra and Bos[5] we were able to aquire the best values for the constants c,a,b for the $0p_{1/2}$ shell via a least square fitting routine.

The following represent the results of these calculations.

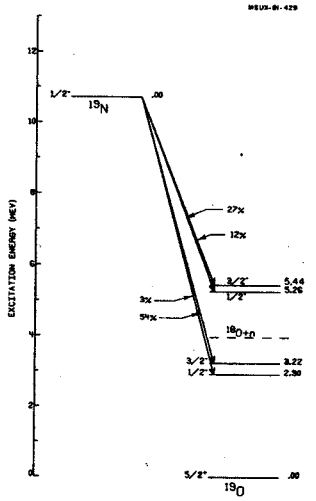

Fig. 1. The decay of $^{19}N(1/2^-)$ to the four dominant G-T allowed states in ^{19}O. The figure indicates that approximately 40% of the G-T transition strength populates neutron unbound states in the daughter nucleus.

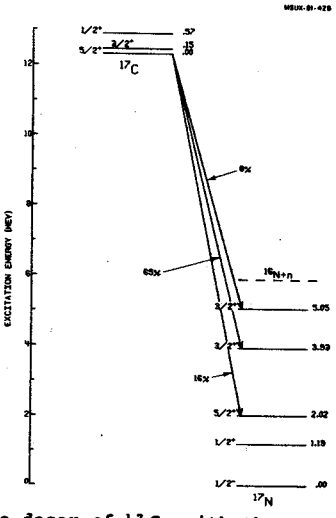

Fig. 2. The decay of ^{17}C, with the assumption of a $5/2^+$ ground state, to the three dominant G-T allowed states in ^{17}N. Approximately 10% of the transition strength is predicted to populate neutron unbound states in ^{17}N.

Conclusion: It is generally felt that the exclusion of the $d_{3/2}$ orbit form the calculation is reflected in too short a life time. This is due to the fact that the $d_{5/2}$ and $d_{3/2}$ contribution's to the GT matrix element come in with different phase, reducing the matrix element and giving a longer lifetime prediction. Calculations are now underway to include the $d_{3/2}$ orbit.

---

1. B.S. Reehall and B.H. Wildenthal, Particles and Nuclei 6 (1973) #6.
2. B.A. Brown, N. Chung, and B.H. Wildenthal PRL 40 (1978) 1631.
3. D.H. Wilkinson and B.E.F. Macefield NP A232 (1974) 58.
4. A. de Shalit and I. Talmi, Nuclear Shell Theory (Academic Press, New York, 1963).

Lifetimes of Exotic sd Shell Nuclei

M.S. Curtin and B.H. Wildenthal

The sd shell model Hamiltonian of Chung and Wildenthal[1] was used to construct ground state wavefunctions of ^{31}Al, ^{32}Al, ^{26}Ne, ^{24}F, ^{25}F, and wavefunctions associated with states of their corresponding daughter nuclei. Gamow-Teller matrix-elements were calculated using free-nucleon single-particle matrix elements following the prescription of Brown, Chung and Wildenthal,[2] from which theoretical $ft_{1/2}$ values were obtained. Finally, calculation of statistical factors using the formalism of Wilkinson and Macefield,[3] yields predictions for theoretical halflives. The strong energy dependence in the statistical factor requires accurate determination of beta decay energies if one is to have confidnece in these theoretical lifetimes. To reduce energy uncertainties associated with the beta decay process, we use Q values from the mass table of Comay and Kelson,[4] and when possible, use experimental daughter state excitation energies of Endt and Van der Leun.[5] Table I presents a comparison between halflives calculated with shell model Q values and excitation energies, and halflives calcualted with the modified Q values and excitation energies. Since the lifetime, Q value, and branching ratios have been empirically determined for the beta decay of ^{31}Al, it provided us with a valuable check on the predictive capabilities of this procedure. According to reference 5, the 2.789 MeV excited state of ^{31}Si is either a $3/2^+$ or $5/2^+$ state. Table II represents the detailed partial halflives to the 4 dominant GT allowed states in ^{31}Si for the beta decay of ^{31}Al. By requiring theoretical branching ratios to match experimental branching ratios we predict the 2.789 excited state in ^{31}Si to be $3/2^+$.

Table I. A comparison between total halflives predicted using shell model Q values and excited state energies (column 1) and total halflives using Comay and Kelson Q values and experimental excitation energies.

Transition	Shell Model Halflives	Modified Halflives
^{26}Ne → ^{26}Na	0.30 (sec)	0.19 (sec)
^{24}F → ^{24}Ne	0.34	0.21
^{25}F → ^{25}Ne	0.17	0.07
^{31}Al → ^{31}Si	0.98	0.32
^{32}Al → ^{32}Si	0.05	0.02

Table II. Presented below are the decay energies, GT matrix elements, partial halflives and predicted branching ratios associated with the beta decay of ^{31}Al($5/2^+$) to the 4 dominant states in ^{31}Si.

$2J_f$	E_β(MeV)	$\lvert B(GT)^{\frac{1}{2}}_{TH} \rvert$	$t_{\frac{1}{2}}$(sec)	B.R.(%)
3.0	7.85	0.45	0.51	63.22
3.0	5.53	0.59	1.56	20.57
5.0	6.15	0.39	2.15	14.89
3.0	5.06	0.18	24.26	1.32

The discrepancy in the theoretical lifetime and the experimental lifetime should diminish when we recalculate the lifetimes using the empirical single-particle matrix elements of the GT operator.

1. W. Chung: Ph.D. Thesis, Michigan State University, unpublished (1976).
2. B.A. Brown, W. Chung and B.H. Wildenthal, Phys. Rev. Lett. 40, (1978) 1631.
3. D.H. Wilkinson and B.E.F. Macefield, NP A232 (1974) 58.
4. Atomic Data and Nuclear Data Tables, Vol. 17 (1979).
5. P.M. Endt and C. Van der Leun, NP A310 (1978) 1.

Shell-Model Calculation of M1 Strength in the Zr Isotopes

N. Anantaraman and B.H. Wildenthal

The recent observation of M1 strength in medium-weight nuclei by inelastic scattering of 200-MeV protons is reported elsewhere in this volume. The excitation energy at which the M1 strength should occur in a spin-unsaturated nucleus can be estimated readily, to zeroth order, from the energy splitting of the single-particle spin-orbit partner levels which couple to form the 1^+ state. For a more accurate estimate of the location and for studying other properties such as the strength and the distribution of the excitation, a detailed shell-model calculation is necessary. We have performed such a calculation for the $^{90\text{-}94}$Zr isotopes.

Only neutron excitations were considered, with ^{80}Zr treated as the core and with the valence neutrons distributed in the $1g_{9/2}$, $2d_{5/2}$, $3s_{1/2}$, $2d_{3/2}$ and $1g_{7/2}$ orbitals, subject to the restriction that the $g_{9/2}$ orbital was occupied by either 9 or 10 particles. This restriction was necessary to reduce the dimensionalities of the problem to manageable levels. The neglect of proton excitations may not be a serious limitation in studying the relative variation of the properties of the excitation over the range of isotopes, since they should all have nearly the same proton character.

The interaction used was of the surface-delta type,

$$V = -4\pi V_0 \delta(\vec{r}_1 - \vec{r}_2).$$

The strength V_0, and the energies of the single-particle levels, were determined by requiring that the low-lying spectra calculated for ^{91}Zr and ^{92}Zr agreed with the known levels of these nuclei. Since only neutron excitations were considered in the calculation, only a subset of the known levels--those having primarily neutron excitation--were used for the comparison. These were identified on the basis of strong population in (d,p) reactions. The single-particle energies thus determined, relative to the ^{90}Zr ground state, were: -11.35 MeV ($g_{9/2}$), -7.2 MeV ($d_{5/2}$), -6.0 MeV ($s_{1/2}$), -5.3 MeV ($d_{3/2}$) and -5.3 MeV ($g_{7/2}$). The strength of the two-body interaction similarly determined was $V_0 = 0.36$ MeV.

The M1 strengths of interest are those corresponding to the transitions G.S.$(0^+) \rightarrow 1^+$ for the even isotopes and G.S.$(5/2^+) \rightarrow 3/2^+$, $5/2^+$ and $7/2^+$ for the odd isotopes. Even though ^{91}Zr is the only stable odd isotope, calculations were also performed for ^{93}Zr, for the sake of studying the systematics. Since only neutron excitations were considered, the M1 operator was proportional to the σ operator (no orbital contribution). The distributions of M1 strength calculated for the various isotopes are shown in Figs. 1 and 2 as a function of the excitation energy of the final state. For ^{92,93,94}Zr, histograms of strengths summed in 0.5 MeV bins are plotted.

The most striking feature of these results is the concentration of M1 strength in a relatively narrow range of excitation in each of the nuclei. The location of this strength, ~ 7.5 MeV, is approximately the same for all the isotopes, in accordance with what is observed in the (p,p') reaction for ^{90,92,94}Zr, but it is about 1 MeV lower than the observed value. It is possible that inclusion of other terms in the residual interaction will remove this difference while leaving the low-lying spectra unaffected.

The calculated widths of the distributions cannot be compared with the data because each state should have a substantial intrinsic width on account of high excitation, and this is ignored in the calculation. But one result shown by the calculation, that the widths are larger for the odd-mass isotopes, can be tested experimentally, provided measurements are made on ^{91}Zr.

In the foregoing discussion, it has been tacitly assumed that the B(M1) strength distribution is an accurate reflection of the cross sections measured in the (p,p') reaction. To test this assumption, microscopic (p,p') calculations were performed for the strongest two 1^+ states in ^{92}Zr, using transition amplitudes obtained from their full shell-model wave functions. It was verified that the ratio of the calculated (p,p') cross sections was the same as the ratio of the B(M1) strengths.

The summed strengths are listed in Table I under the columns Σ_{n_f} B(M1) and Σ_{d_f} B(M1). n_f is the number of final states for which calculations were actually carried out; for the heavier isotopes, this is a small fraction of the total number of possible states, which equals the dimensionality d_f. The sum Σ_{n_f} B(M1) is obtained by adding all the calculated strengths, while Σ_{d_f} B(M1) is obtained by use of a closure relation applied to the ground states. The last column, Σ_{d_f} B(M1: SSM G.S.), lists the results of the closure relation obtained using alternative ground-state wave functions corresponding to the simple shell model (SSM) limit, constructed by assigning the dominant component of the full ground state eigenvectors an amplitude of 1.0.

There are several points to notice in Table I. (i) Even though practicality restricted us to a small fraction of final states in the case of ^{93,94}Zr, a major portion of the total M1 strength is located in these states. Thus the location and width of the distributions for ^{93,94}Zr are

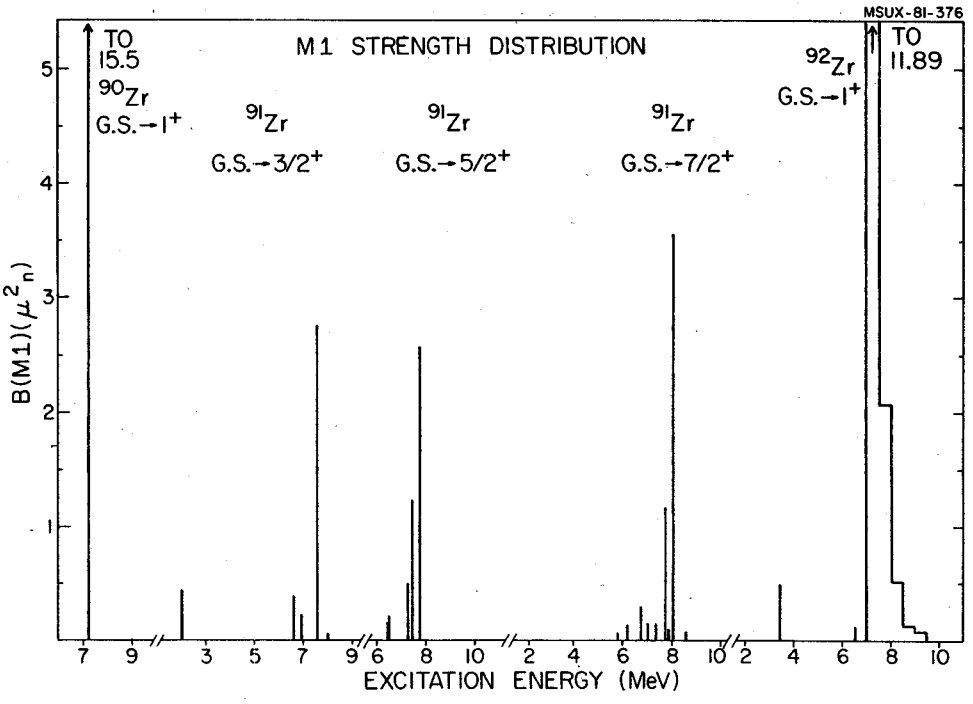

Fig. 1. Distributions of M1 strengths calculated for transitions from the ground states of ^{90,91,92}Zr to excited states.

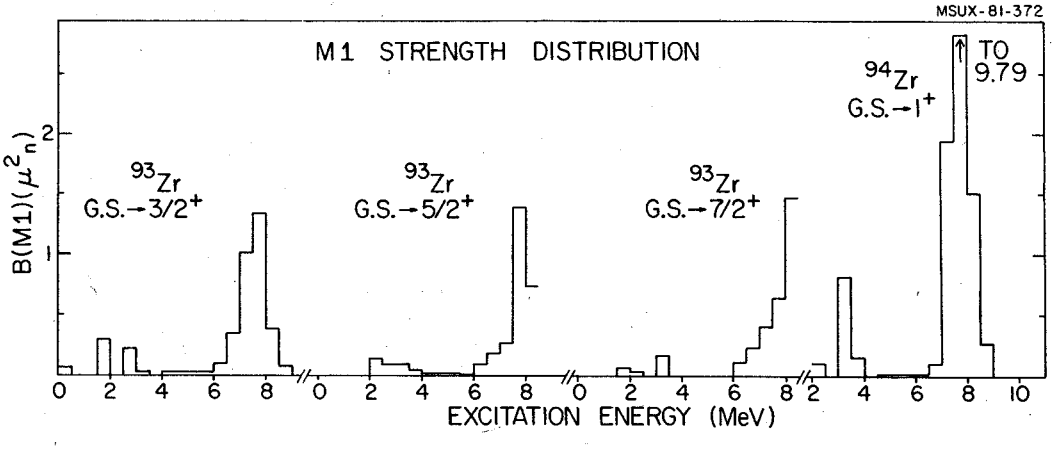

Fig. 2. Distributions of M1 strengths calculated for transitions from the ground states of ^{93,94}Zr to excited states.

Table I. M1 Strengths in the Zr Isotopes.

Nucleus	Transition	n_f	d_f	$\Sigma_{n_f} B(M1)$ (μ_n^2)	$\Sigma_{d_f} B(M1)$ (μ_n^2)	$\Sigma_{d_f} B(M1:SSM\ G.S.)$ (μ_n^2)
^{90}Zr	G.S. → 1^+	1	1	15.50	15.50	15.50
^{91}Zr	G.S. → $3/2^+$	16	16	3.98	3.98	4.84
	→ $5/2^{+*}$	23	23	4.92	4.92	5.54
	→ $7/2^+$	27	27	6.09	6.09	6.89
^{92}Zr	G.S. → 1^+	24	69	15.34	15.48	18.29
^{93}Zr	G.S. → $3/2^+$	66	346	3.85	3.95	5.03
	→ $5/2^{+*}$	66	474	3.67	5.75	7.43
	→ $7/2^+$	66	550	3.18	6.25	7.82
^{94}Zr	G.S. → 1^+	66	788	14.83	15.57	21.09

*Excluding G.S. → G.S. transition!

calculated reliably, despite the restriction just mentioned. (ii) The constancy of the total strength $\Sigma_{d_f} B(M1)$ is a remarkable result which is not intuitively obvious. (iii) The effect of correlations in the ground state can be studied by comparing the numbers in the last two columns of Table I. It is seen that the effect of the correlations is to progressively reduce the M1 strength as one goes to the heavier isotopes. In the case of ^{94}Zr, the full shell-model strength is quenched by about 25% relative to the simple-configuration value.

An Effective Interaction for Inelastic Scattering Derived From the Paris Potential

N. Anantaraman, H. Toki and G. Bertsch

Some years ago, Bertsch et al.[1] derived from the phenomenological Hamada-Johnston and Reid nucleon-nucleon (N-N) potentials effective interactions for inelastic nucleon scattering. In the present work, a similar procedure has been carried out starting with the Paris N-N potential, an analytic parameterization of which became available recently.[2] New phase-shift data obtained in the 1970's went into the development of this potential, and it is based on a more fundamental theory of the N-N interaction than the earlier potentials. These reasons motivated us to study whether the effective matrix elements derived from it differed in any significant respect from those of ref. 1.

From the Paris N-N potential, G-matrix elements in the harmonic oscillator basis were obtained by the method of Barrett et al.[3] This consisted in solving the Schrodinger equation

$$\left(E + \frac{\hbar^2}{m}\nabla^2 - \frac{1}{4}m\omega^2 r^2 - V(r)\right)\psi = 0$$

for eigenerengy E and eigenfunction ψ in various two-nucleon channels ($^1S_0$, $^3P_1$, etc.). For the $^3S_1$ and $^3D_1$ channels, which are coupled by the tensor part of the potential, a set of coupled differential equations was solved. ψ has a high degree of overlap with some oscillator function ϕ_{nl}. The free G-matrix elements were then obtained from the relation

$$G^{o}_{nl} = \langle\phi_{nl}|G|\phi_{nl}\rangle = E - E_{nl} \ ,$$

where E_{nl} is the oscillator energy in state ϕ_{nl}.

Because of the energy dependence of the Paris potential, the computer programming required was more complicated than for the potentials used in ref. 1. It was tested by calculating the phase shifts in the uncoupled channels and verifying that they agreed with the values reported in ref. 2. For the $^3S_1$-$^3D_1$ calculation, it was verified that the deuteron binding energy and wave function were correctly reproduced.

The next step was to correct the free G-matrix elements for the Pauli blocking effect by introducing an energy gap of 40 MeV between occupied and unoccupied orbits.[3] The resulting effective G-matrix elements are listed in Talbe I. They agree for the most part to within 10% with the values obtained from the Reid potential (see Table 3 of ref. 1). Only in the case of the column headed n=3 for the SE channel are there significant differences. But, since they occur mainly for highly nondiagonal matrix elements, these differences do not noticeably affect inelastic scattering results.

Table I. Oscillator G-matrix elements of the Paris potential in MeV ($\hbar\omega$ = 14 MeV).

	S/S	n = 0	1	2	3
	n' = 0	-6.73	-5.27	-3.73	-11.28
Singlet	1		-4.84	-3.47	-6.46
Even	2			-2.61	-1.44
	3				2.51
	S/S	n = 0	1	2	3
	n' = 0	-9.63	-8.90	-7.55	-6.07
Triplet	1		-8.43	-6.82	-5.63
Even	2			-5.83	-5.02
	3				-2.82
	P/P	n = 0	1	2	3
	n' = 0	2.52	2.37	2.11	1.89
Singlet	1		3.03	3.00	2.81
Odd	2			3.39	3.41
	3				3.74
	P/P	n = 0	1	2	3
	n' = 0	-0.08	-0.23	-0.09	-0.05
Triplet	1		-0.24	-0.05	0.01
Odd	2			0.04	0.13
	3				0.31
	S/D	n = 0	1	2	3
	n' = 0	-5.54	-7.62	-8.66	-9.21
Tensor	1	-2.61	-5.09	-6.90	-8.11
Even	2	-1.35	-2.95	-4.72	-6.23
	3	-0.72	-1.66	-2.98	-4.39
	P/P	n = 0	1	2	3
	n' = 0	0.78	0.75	0.63	0.54
Tensor	1		0.92	0.87	0.79
Odd	2			0.95	0.93
	3				1.00
	D/D	n = 0	1	2	
	n' = 0	-0.14	-0.13	-0.12	-.21
LS	1		-0.18	-0.21	-.47
Even	2			-0.26	-.70
	3				-.91
	P/P	n = 0	1	2	3
	n' = 0	-0.57	-0.90	-0.96	-1.06
LS	1		-1.28	-1.40	-1.55
Odd	2			-1.71	-1.91
	3				-2.19

These matrix elements can be used in different applications, such as nuclear structure calculations and the extraction of the parameters of the Landau-Migdal force. Here we focus on the application to inelastic nucleon scattering. A least-squares fitting of the effective G-matrix elements in the various channels to a set of Yukawa potentials with at most four ranges was performed. This was because the distorted-wave inelastic scattering program DWBA-70[4] can handle a sum of central, tensor and spin-orbit components specified in the form of a superposition of Yukawas of four different ranges. (Actually, the form of the

tensor part is $r^2Y(r)$.) The choice of the ranges was physically motivated, as discussed in ref. 1, and consisted of 0.25, 0.4, 0.7 and 1.414 fm. The one-pion exchange potential tail was imposed on the central part of the interaction.

The results are shown in Table II where, for each channel, two rows of interaction strengths are given. The first row is that derived from the Paris potential, the second that from the Reid potential. The similarity of numbers in the two rows is noteworthy. It indicates that the differences that exist between the theoretically motivated Paris potential and the earlier, phenomenological potentials, will not show up in inelastic scattering results.

To test this reasoning, inelastic scattering cross sections were computed with the microscopic code DWBA-70 for various levels excited in the ^{24}Mg(p,p') reaction. Zwieglinski et al.[5] have studied this reaction experimentally at 40 MeV and also analyzed it microscopically using a particular choice of the interactions given in ref. 1. We repeated this analysis, and also did similar calculations using the two sets of interaction listed in Table II. The shapes of the angular distributions calculated with all three sets of interaction are identical, and the normalizations (N) between the measured and calculated cross sections are similar. Table III lists the values of N obtained for some of the states in ^{24}Mg. For all three interactions, these are quite similar--in both T=0 and T=1 channels, and for both spin-flip (odd J) and non-spin-flip (even J) transitions. Thus we conclude that the effective interaction for inelastic scattering obtained form the Paris potential is very similar to those derived from the earlier, phenomenological potentials.

Table III. Normalizations for levels populated in ^{24}Mg (p,p') at 40 MeV.

$J^\pi T$	N_{Reid}	N_{Paris}	$N_{Zwieglinski}$[a]
2^+0	2.67	2.74	3.89
3^+0	4.83	4.95	6.04
2^+1	2.64	2.69	3.20
3^+1	1.69	1.67	1.82

a) Values obtained using the interaction and method of ref. 5 but with normalizations done by the present authors.

1. G. Bertsch et al., Nucl. Phys. A284, 399 (1977).
2. M. Lacombe et al., Phys. Rev. C21, 861 (1980).
3. B. Barrett et al., Phys. Rev. C3, 1137 (1971).
4. R. Schaeffer and J. Raynal, unpublished.
5. B. Zwieglinski et al., Phys. Rev. C18, 1228 (1978).

Table II. Best Fit Interaction Strengths in MeV

Channel	Name	R_1 = 0.25 fm	R_2 = 0.40 fm	R_3 = 0.7 fm	R_4 = 1.414 fm
SE	Paris	11466.	-3556.		-10.463
	Reid	12455.	-3835.		-10.463
TE	Paris	13967.	-4594.		-10.463
	Reid	21227.	-6622.		-10.463
SO	Paris	-1418.	950.		31.389
	Reid	29580.	-3464.		31.389
TO	Paris	11345.	-1900.		3.488
	Reid	12052.	-1990.		3.488
TNE	Paris		-1096.	-30.9	
	Reid		-1260.	-28.4	
TNO	Paris		244.	15.6	
	Reid		263.	13.8	
LSE	Paris	-5101.	-337.		
	Reid	-4382.	-352.		
LSO	Paris	-1897.	-632.		
	Reid	-2918.	-483.		

The Schematic Model for odd-A Nuclei

J. Ginocchio* and O. Scholten

One of the basic assumptions in the IBA model is that the low-lying collective states can be described in terms of pairs of particles coupled to angular momentum J=0 or 2. In a realistic shell model calculation this is true to a great extent. Recently Ginocchio[1] has introduced a model, called the Schematic Model, in which the IBA sector (formed by products of a collective J=0 and a J=2 state) of the basis is completely disjoint. One can make therefore an exact correspondence between the states in the fermion and those in the boson model. This exact relation allows one to study in detail the mapping of operators from the fermion space into the IBA boson space, taking the two particle structure of the bosons correctly into account.

The correspondence between the Schematic model and the boson model has only been formulated explicitly[1] for the case of an even number of fermions. However especially odd A nuclei are interesting to study since the effect of the Pauli principle (blocking) is extremely important. We are therefore extending the method to odd-systems which turns out to be non trivial. Of special interest is the operator for single particle transfer.

---

* LASL, Los Alamos, NM 87545.

1. J.N. Ginocchio, Ann. of Phys. 126 (1980) 234.

A Microscopic Approach to the IBA Model

O. Scholten

In the IBA model the low-lying collective states in heavy and medium heavy nuclei are described in terms of a system of interacting s and d bosons. A boson is regarded as a collective two particle state,

$$s^+ \leftrightarrow \tfrac{1}{2}\sum_j \alpha_j \hat{j}(c_j^+ c_j^+)^{(0)} \tag{1a}$$

$$d_m^+ \leftrightarrow \sum_{j\,j'} \beta_{jj'} \frac{1}{1+\delta_{jj'}} (c_j^+ c_{j'}^+)_m^{(2)} \tag{1b}$$

where the summation runs over spherical shell model states. One of the open problems in the IBA approach is the calculation of the s and d boson structure coefficients α_j and $\beta_{jj'}$ from a microscopic model. This is especially important for odd-A nuclei since they appear explicitly in the calculation.[3]

The coefficients α_j and $\beta_{jj'}$, should in principle be calculated from a diagonalization of the Hamiltonian in a full shell model basis. For the nuclei we are interested in the size of the matrices to be diagonalised is however prohibitive. In an alternative approach we will treat the neutrons and protons separately. In the shell model the separate treatment of the neutron and proton degrees of freedom reduces the dimension from about 10^{14} to 10^5 for a typical medium heavy nucleus. In the present approach we will reduce the dimensionality of the problem even further to about 20. The Hamiltonian which we use as a starting point is:

$$H = H_\pi + H_\phi + \kappa Q_\pi^{(2)} Q^{(2)} + V_{\pi\pi} + V_{\nu\nu} \tag{2}$$

where

$$H = \sum_j \epsilon_j n_j + \frac{G}{4} \sum_{jj'} \hat{j}\hat{j}' (c_j^+ c_{j'}^+)^{(0)} (\hat{c}_j \hat{c}_{j'})^{(0)} \tag{3a}$$

and

$$Q_m^{(2)} = \sum_{jj'} q_{jj'} (c_j^+ \hat{c}_{j'})_m^{(2)}. \tag{3b}$$

As has been pointed out by Talmi[1] the resiudal interaction between like fermions, $V_{\pi\pi}$ and $V_{\nu\nu}$, conserve seniority. Since we will truncate our space at $v = 2$, $J = 2$, V is imply taken equally attractive for all $J = 2$ states.

$$V = V_2 \sum_{jj'} (c_j^+ c_{j'}^+)^{(2)} \cdot (\hat{c}_j \hat{c}_{j'})^{(2)} \tag{3c}$$

To determine the structure coefficients of the bosons we will take an iterative approach. To solve the problem for the proton bosons we will assume that the neutron sector has already been solved which means that we can diagonalise the Hamiltonian(2) in the space spanned by

$$|\, s_\nu^{N_\nu} >,\ |\, s_\nu^{N_\nu - 1}\, d_\nu > \tag{4a}$$

in the neutron sector and

$$|\, s_\pi^{N_\pi} >,\ |\, s_\pi^{N_\pi - 1}\, (jj')^{(2)} > \tag{4b}$$

for the protons. In eq. (4) the number of bosons is half the number of fermions, N=n/2. In the J=2 states in eq. (4.b) two fermions are coupled to angular momentum 2 and as a consequence there are only N-1 bosons.

The calculation of the matrixe elements of the Hamiltonian, eq. (2), in the basis (4) can be done as proposed, by Otsuka.[2] We will take here a slightly different approach which is simpler but introduces more approximations. The pure neutron part of the Hamiltonian can be replaced by $\epsilon_d n_d$ apart from an overall constant. In the evaluation of the proton part one must however take into account that the fermion operators c_j^+ do not commute with the bosons,

$$[s,\ c_{jm}^+] = \alpha_j c_{jm} \tag{5}$$

The Hamiltonian can be put in a more transparent form by introducing the quasi-particle operators a_{jm}^+, which by definition commute with the boson operators. One can express the fermion operators in terms of these quasi-particles, giving in lowest order[3]

$$c_{jm}^+ \simeq u_j a_{jm}^+ + \frac{v_j}{N} s^+ \hat{a}_j\ , \tag{6}$$

where u_j and $u_j = 1 - v_j^2$ are introduced in analogy with BCS. In this case the v_j are related to the s boson as $v_j = \sqrt{N}\alpha_j$. It can easily be shown that $v_j^2 = \langle s^N | n_j | s^N \rangle / (2j+1)$ as implied by the occupation probability interpretation. If we simply substitute eq. (6) in eq. (2) and keep only the terms that will not vanish for the states under consideration we obtain, apart from an overall constant

$$\begin{aligned} H = {} & \epsilon_{d\nu}\, n_{d\nu} + N\epsilon_s + \sum_j (u_j^2 - v_j^2)\hat{j}\epsilon_j n_j^q + V_{\pi\pi} + \\ & - \frac{G}{4}\sum_{jj'} \hat{j}\hat{j}' (u_j v_j u_{j'} v_{j'} \hat{j}\hat{j}' + 2 v_j^4 \delta_{jj'}) + \\ & + G\sum_j \left(v_j^4 + \sum_{j'} (u_j u_{j'} (2j+1) u_j v_j) n_j^q\right) + \\ & - G \left(\sum_j u_j v_j n_j^q\right)^2 + \\ & + K' Q_{\nu jj'} q_{jj'} \frac{u_j v_{j'} + v_j u_{j'}}{2\sqrt{N}} (s a_j^+ a_{j'}^+)^{(2)} + \text{h.c.}) \end{aligned}$$

$$+ K'Q_{\nu} \sum_{jj'} q_{jj'}(v_j v_{j'} - u_j u_{j'})\,(a_j^+ \hat{a}_{j'})^{(2)}$$

where n_j^q is the quasi-particle number operator, K' and ϵ_{d_ν} can be calculated from the structure of the neutron bosons and

$$\epsilon_s = \Sigma_j \epsilon_j v_j^2 (2j+1)/N \quad , \tag{8}$$

$$\hat{\epsilon}_j = \epsilon_j - \epsilon_s/2 \; . \tag{9}$$

The Hamiltonian eq. (7) is similar to the BCS Hamiltonian.[4] However, by introducing quasi-particles in the BCS formalism we are faced with the problem of the violation of number conservation. For a single j-shell this shows up by the fact that the matrix element of the number operator equals $2N + (u_j^2 - v_j^2)$. Also in the present approach we can see the same symptoms. The origin is however completely different. In the approach of Otsuka,[2] which is closer to the exact solution, we obtain for the image of the number operator

$$n_j = \frac{1}{v_j^2}\left(\sum_{j'} v_{j'}^2 (2j'+1) + (u_j^2 - v_j^2 - \frac{v_j^2}{N})\right) n_j^q \tag{10}$$

which obeys $\Sigma n_j = 2N+1$. By comparing with eq. (7) it can be seen that the present approach corresponds to the approximation $v_j^2/N \ll 1$. From eq. (10) it can also be seen that the gauge transformation (eq. 9) is necessary to obtain the correct quasiparticle energies. The Hamiltonian eq. (8) can be diagonalised numerically. The coefficients ϵ_j can be determined by minimizing the energy of the 0_1^+ state. The coefficients $\beta_{jj'}$ follow from the structure of the 0_2^+ or 2_1^+ state in this basis. With this structure coefficients one can calculate the parameters of the IBA model.

It should be noted that the present approach is valid for spherical as well as deformed nuclei. Contrary to what is attempted in other models, such as RPA we are not calculating the actual nuclear ground or 2_1^+ state, but only the parameters for the boson-boson interaction. The nuclear states follow from the IBA calculation.

---

1. I. Talmi, In "Interacting Bosons in Nuclear Physics", F. Iachello ed., Plenum Press, New York (1979) p. 79.
2. T. Otsuka, Ph.D. Thesis, University of Tokyo, Japan (1979).
3. O. Scholten, Ph.D. Thesis, University of Groningen, The Netherlands, (1980).
4. A.M. Lane, "Nuclear Theory", W.A. Benjamin, New York (1964).

A Pseudo-Spin Symmetry in the IBFA Model

O. Scholten

In some medium-heavy odd-A nuclei a striking doubling of levels, with spins J and J-1, have been observed. In the IBFA[1,2] model this can easily be explained in terms of a pseudo-spin symmetry. The exact symmetry occurs in the IBFA Hamiltonian whenever the odd-fermion can occupy two single particle (s.p.) orbits, which differ in spin by one unit and have equal s.p. energies and thus also equal occupation probabilities. The orbital angular momenta can be different.

The symmetry is most easily worked out in the ℓ-s rather than the usual j-j coupling scheme. The relation between the two is given by

$$|\alpha,(R,\ell)L,1/2;\ J> = \sum_{j=\ell-1/2}^{\ell+1/2} (-1)^{R+\ell+J+1/2} \sqrt{(2L+1)(2j+1)} \begin{Bmatrix} R & \ell & L \\ 1/2 & J & j \end{Bmatrix} |\alpha,R,(\ell,1/2)j;J> \qquad (1)$$

where R is the boson total angular momentum and α denotes the other quantum numbers necessary to label the boson state uniquely. The ℓ introduced in Eq. (1) is not necessarily the real s.p. orbital angular momentum, but is chosen such that the j-values of the two involved s.p. orbits can be obtained from it by coupling a pseudo-spin, i.e. $\ell = (j + j')/2$. The symmetry is based on the fact that in the IBFA model the boson fermion interaction stems from a nucleon-nucleon quadrupole force which acts only on the pseudo-orbital angular momentum. Because of the spin independence of the interaction, the energies depend only on $(\ell,(R,\ell)L)$ and the levels in the spectrum thus occur in doublets with spins $J = L \pm 1/2$.

Although unequal occupation probabilities or unequal s.p. energies break the symmetry, still several examples can be found. In Fig. 1 the positive parity spectra of ^{151}Eu and ^{153}Eu are shown, in which the odd proton occupies the close lying 1d 5/2 and 0g 7/2 orbits.

The present symmetry predicts also a simple selection rule for single particle transfer, namely that levels with $L \neq \ell$ will not be excited. As an example the measured spectroscopic factors for ^{151}Eu and ^{153}Eu are given in Fig. 1. No state with $L \neq \ell=3$ is strongly excited. The nicest example is the g.s. of ^{153}Eu which is not excited in $d_{5/2}$ transfer although it is the lowest $5/2^+$ state.

In the symmetry discussed here the actual strcuture of the even-even case does not enter, it is entirely related to the odd-particle. In this respect it should be distinguished from the super-symmetries discussed in Ref. 3.

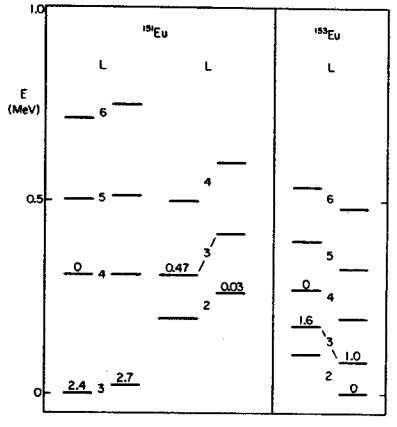

Fig. 1. The levels in the positive parity spectrum of ^{151}Eu[4] and ^{153}Eu[5] have been ordered in doublets on the basis of excitation energies and spin assignments. It is furthermore assumed that the pseudo-angular momentum, L, increases for the levels in an experimentally well established band. For each doublet the value of L is given, the level with $J = L - 1/2$ is plotted on the left and $J = L + 1/2$ on the right. The value of the d 5/2 and g 7/2 spectroscopic factor as measured in $(^3He,d)$[6,7] is also given in the figure.

1. F. Iachello and O. Scholten, Phys. Rev. Lett. 43 (1979) 679.
2. O. Scholten, Ph.D. Thesis, University of Groningen, Groningen, The Netherlands (1980).
3. F. Iachello, Phys. Rev. Lett. 44 (1980) 772.
4. G. LoBianco, N. Molho, A. Moroni, S. Angius, N. Blasi and A. Ferrero, J. Phys. G5 (1979) 697.
5. C.M. Lederer and V.S. Shirley, "Table of Isotopes", Wiley, N.Y. (1978).
6. O. Straume, G. Løvhøiden and D.G. Burke, Nucl. Phys. A266 (1976) 390.
7. J. Ungrin, D.G. Burke, M.W. Johns and W.P. Alford, Nucl. Phys. A132 (1969) 322.

Forward Angle Inelastic Scattering

G. Bertsch and O. Scholten

Inelastic scattering reactions are particularly interesting at forward angles because the low momentum transfer probes the collective response of nuclei to external fields. The collective cross-section is however obscured by a background which we would like to understand better. We have investigated the one step contribution to this background and shown that it accounts for the cross-section below 40 MeV excitation as observed in proton induced reactions at 200 and 800 MeV.[1]

The double differential cross-section is facotrized as

$$\frac{d^2\sigma}{d\Omega dE} = \frac{d\sigma}{d\Omega}\Big|_{NN} N_{eff}\, S(q,E) \qquad (1)$$

where $\frac{d\sigma}{d\Omega}|_{NN}$ is the nucleon-nucleon cross-section at the same lab energy and angle, N_{eff} is the effective number of participating particles and $S(q,E)$ is the normalized response function.

The effective number of nucleons is calculated as

$$N_{eff} = \sigma^{(1)}/\sigma_{NN} \qquad (2)$$

where $\sigma^{(1)}$ is the total cross-section for single collision scattering and can be calculated using Glauber[2] theory.

In the Fermi gas model for an infinite medium the response function can easily be calculated giving the imaginary part of the Linhard function.[3] This response function is in variance with the data in two respects: i) Considered as a function of E at a fixed value of q, S(q,E) is nearly triangular in shape for small values of q as is shown in Fig. 1. ii) At small momentum transfer, for a given excitation energy, S(q,E) vanishes, while much of the data appear to be independent of q in the forward direction. To improve on these, a better approximation is needed which takes explicitly the nuclear surface into account.

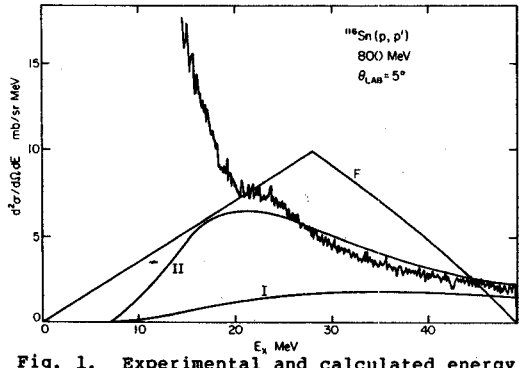

Fig. 1. Experimental and calculated energy spectra for 800 MeV (p,p') on ^{116}Sn at 5° lab. angle; curve F gives the Fermi gas model prediction, curve I is the cross-section for direct knock and II is the cross section leading to unbound states.

Calculations in Glauber theory show that the inside of the nucleus does not contribute to the single collision scattering. To conveniently model the surface we consider a semi infinite slab of nuclear matter. The single particle wave functions are constructed in the potential

$$V(r) = V_o/(1+e^{z/a}) \qquad (3)$$

using V_o = -45 MeV and a = 0.75 fm. The fact that the reaction takes place only at the surface is expressed by including explicitly a cut-off factor in the scattering operator

$$O(q,r) = e^{iqr}/(1+e^{(z-z_o)/a_o})^{\frac{1}{2}} \qquad (4)$$

For the case of 800 MeV protons we obtain z_o = -0.6 fm and a_o = 0.4 fm by fitting $d\sigma^{(1)}/db$ as can be calculated from Glauber theory. In an actual nucleus the transferred momentum q can take all possible orientations Φ with respect to the surface, depending on the azimuthal angle of the surface element. This we account for by averaging over Φ. This procedure can be justified by the fact that experimentally in the angular distribution of the background cross section no interference patterns have been observed. Using energy and momentum conservation to eliminate some of the intergrals, we obtain

$$S(q,E) = \frac{2m}{\pi 3}\int_o^{\pi} d\psi \int dk_z dk_x \sqrt{\frac{k_F^2-k_x^2-k_z^2}{((k_z')^2-2mV_o)}}\; |\langle\psi(k,z)|\theta(q,z)|\psi'(k',z)\rangle|^2 \times \frac{}{\int_o^{k_F} dk_z (k_F^2-k_z^2)\langle\psi(k,z)|^*(q,z)(q,z)|\psi(k,z)} \qquad (5)$$

The momenta k and k' of the bond and scattering state are related by energy and momentum conservation as

$$k_z'^2 = k_z^2 + k_x^2 + 2m(E+V_o) - (k_x+q\sin\phi)^2 \qquad (6)$$

We have numerically evaluated the response function for two cases: 1) $k_z'^2 > 0$, which corresponds to the knock-out process in which the nucleon escapes from the surface (curve I in Figs. 1,2). ii) $k'^2 \geq 0$ corresponding to the scattering of the knocked-on nucleon to unbound states (curve II in Figs. 1,2). The latter explains the data well with the exception of the very forward angles where it underestimates the amount of Pauli blocking. It is shown that direct knock out (curve I) accounts only for a fraction of the cross section below 40 MeV excitation, only at higher excitation energies it forms a substantial contribution to the background.

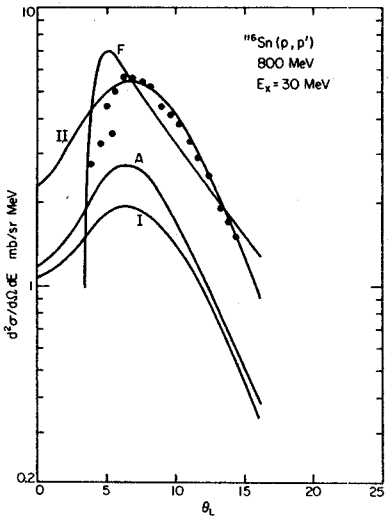

Fig. 2. Experimental and calculated angular distribution for 800 MeV (p,p') on ^{116}Sn at E_x = 30 MeV. The curve labels have the same meaning as in Fig. 1. Curve A follows from an analytic formula not discussed here.

A detailed account of this work in in progress.

---

1. G.F. Bertsch and O. Scholten, Preprint.
2. R.J. Glauber and G. Matthiae, Nucl. Phys. B21 (1970) 135.
3. J. Lindhard, Mat. Fys. Medd. Dan Vid. Selsk 28 (1954) no 8.
4. J. Moss, Private Communication.

Determination of the Landau Parameter g' from the Giant Gamow-Teller States

H. Toki

The recently obtained (p,n) data on the giant Gamow-Teller states in heavy double closed shell nuclei are used to extract the Landau parameter g', the strength of the particle-hole interaction in the spin-isospin channel at zero momentum transfer (q=0). We take one and two pion exchanges in addition to the Landau term as the residual interaction and determine the strength g' from the excitation energies of the giant Gamow-Teller states in the neighboring nuclei of ^{48}Ca and ^{90}Zr.

We take the Woods-Saxon potential for the radial wave functions and the spin-orbit splitting from the optical model analysis of Becchetti and Greenless. Using the excitation energies of the Gamow-Teller states; E_x = 10.4 MeV for ^{48}Ca and E_x = 8.7 MeV for ^{90}Zr, we obtain g' = 0.55 for ^{48}Ca and g' = 0.40 for ^{90}Zr with the zero-range interaction. The addition of the V_π and $V_{2\pi}$ substantially increases these values to g' = 0.77 for ^{48}Ca and 0.61 for ^{90}Zr. Furthermore, we have considered the exchange term of the one pion exchange and found that this term has only a little effect on the value of g'. The inclusion of the finite range interaction improves the excitation energies and the transition strengths for the lower M1 states.

The present investigation suggests that the Landau parameter g' might have a large mass dependence even after about 10% errors are allowed for g' due to the experimental determination of the excitation energies and the 1.s splitting energy. This trend might be supported by the similar calculation of Krewald et al. performed in the ^{208}Pb region.[1] They obtain g' = 0.50, the value of which is converted from g'_0 = 0.65 to the present unit.

---

1. S. Krewald, F. Osterfeld, J. Speth and G.E. Brown, Phys. Rev. Lett. 46 (1981) 103.

Quenching of Magnetic Transitions in ^{48}Ca

H. Toki, A. Harting,* W. Weise* and A. Richter**

We apply the quenching mechanism of the magnetic transitions via the Δisobar-hole intermediate excitations to the case of the $J^\pi = 1^+$ state at $E_x = 10.23$ MeV in ^{48}Ca.[1] The recent backward (e,e') measurement yielded $B(M1) = (4.0 \pm 0.3)\mu_N^2$, which is considerably small as compared to the simple shell model prediction $B(M1) = 12.0\mu_N^2$.[2]

The M1 operator is

$$T_{1M}(q,\vec{r};\vec{\sigma}) = i\frac{q}{2M}\sum_{L=0,2} b_{1L} M_{1LM}(q,\vec{r};\vec{\sigma})(\mu_s+\tau_3\mu_v) \quad (1)$$

$$M_{1LM}(q,\vec{r};\vec{\sigma}) = i^L j_L(qr)\vec{Y}_{1LM}(\hat{r})\cdot\vec{\sigma} \quad (1a)$$

where $b_{10} = \sqrt{2/3}$, $b_{12} = \sqrt{1/3}$, $\mu_s = 0.44\mu_N$, $\mu_v = 2.35\mu_N$, Y_{1LM} are vector spherical harmonics. In the presence of virtual Δ-hole excitations, the isovector part of the M1 operator is renormalized as

$$\tilde{M}_{1L}(q,\vec{r};\vec{\sigma})\tau_3 = \sum_{L'=0,2}\int_0^\infty \frac{dk k^2}{(2\pi)^3} M_{1L'}(k,\vec{r};\vec{\sigma})\tau_3 \hat{\mu}_{J=1}^{L,L'}(k,q) \quad (2)$$

where the polarization tensor $\hat{\mu}_{J=1}^{L,L'}(k,q)$ is obtained through the Δ-isobar hole excitations mediated by the Δ-hole interaction

$$W(q) = \frac{f^{*2}}{m_\pi^2}(V_\pi(q)\vec{S}_1^+\vec{q}\,\vec{S}_2\vec{q} + V_\rho(q)\vec{S}_1^+\vec{x}\vec{q}\cdot\vec{S}_2\vec{x}\vec{q} \quad (3)$$
$$+ g'\vec{S}_1\cdot\vec{S}_2)\vec{T}_1\cdot\vec{T}_2$$

we take the Chew-Low relation $f^{*2}/4 = 4f^2/4 = 0.32$.

Calculated results for the Δ-induced quenching effect on the shell-model B(M1) value are presented in Fig. 1. Here the correlation parameter g' has been varied within a reasonalbe range; $0.5 \lesssim g' \lesssim 0.7$. With $g' \sim 0.55$, the B(M1) value is quenched by about a factor of two.

We demonstrated that a large fraction of the quenching strength is due to the Δisobar excitation. The remaining piece of the required quenching may be traced back to open-shell components which reduce the weight of the $(f_{5/2}f_{7/2}^{-1})$ combination, although not by a very large amount.[3] In fact, the high resolution ^{48}Ca (e,e') experiment has identified several weak M1 states in the vicinity of the $E_x = 10.23$ MeV state.[4] The total experimental strength is $\Sigma B(M1) \simeq 5.2\mu_N^2$ and is very close to the prediction of the Δ-hole polarization as shown in Fig. 1.

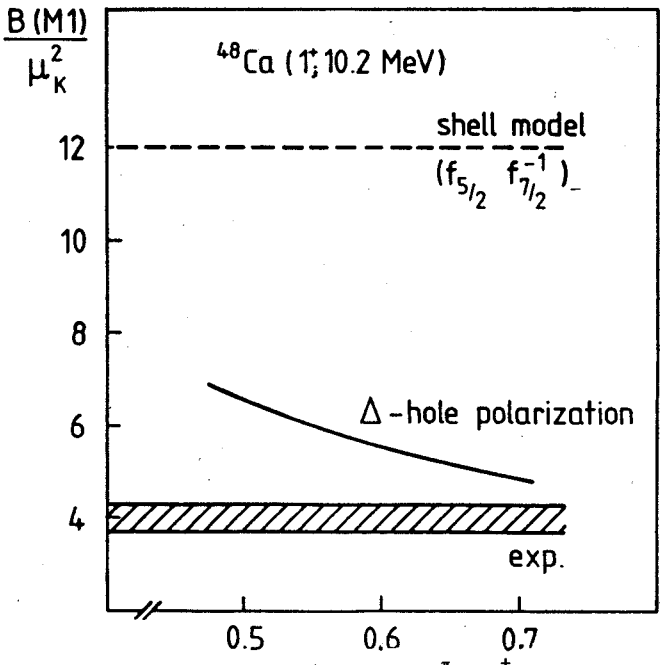

Fig. 1. The B(M1) value for the $J^\pi = 1^+$ state at $E_x = 10.23$ MeV in ^{48}Ca. The calculated results with the isobar-induced quenching effect are shown by the solid line as a function of the Landau parameter g'.

* University of Regensburg, Regensburg, W. Germany.
** Technin sche Hochschule Darmstadt, Darmstadt, W. Germany.

1. A. Harting, W. Weise, H. Toki and A. Richter, Phys. Lett. (1981).
2. W. Steffen, et al., Phys. Lett. 95B (1981).
3. J.B. McGrory and B.H. Wildenthal, preprint (1981).
4. W. Steffen, et al., to be published.

The Beta Decay of ^{145}Gd

D. Cha and G. Bertsch

Nuclear response theory, as developed by Bertsch and Tsai[1] has recently been applied[2] to the charge exchange reaction for the $\sigma\tau$ strength, and shows good agreement with the data in the whole range of medium and heavy nuclei. This encourages us to try it on Gamow-Teller beta decays. Due to the large population of the final states in the decay of heavier nuclei, there has been few sophisticated calculations of the beta strength function. It is commonly assumed that the strength is a smooth function peaked at the position of the Gamow-Teller giant state.[3] However, most phenomena associated with beta decay depend only on the low-lying part of the strength function. Klapdor and Wene pointed out in their recent review article[4] that the presence of structure in the low-lying strength function can have a strong effect on the predictions. The nuclear response theory can deal effectively with the large space of exciations possible in medium and heavy nuclei, so it should be useful in the calculation of structure in the low-lying strength function.

A good example of a beta decay strength function which exhibits structure is the beta decay ^{145}Gd → ^{145}Eu. The data of Firestone et al.[5] show concentrations of β^+ decay strength at 1.04, 1.82, 2.48 and 4.50 MeV in the daughter nucleus. In this work, we adopt the same model as Ref. 2, namely the TDA based on either Woods-Saxon or Skyrme Hartree-Fock wavefunctions. In addition, we introduce pairing correlations in the ground state. The pure Hartree-Fock shell model does not allow the decay of ^{145}Gd because all the neutron levels energetically accessible for this transition are already filled. We therefore modified the theory by including pairing correlations in the ground state. We also use a simple delta-function as a residual interaction with the strengths of 220 MeV-fm^3 for Woods-Saxon and 200 MeV-fm^3 for Hartree-Fock single particle spectra. These are determined by the giant Gamow-Teller strength of the (p,n) reaction in Ref. 2. It has been shown by Halbleib and Sorenson[6] that individual Gamow-Teller beta decay transition rates in medium-heavy spherical nuclei can be well represented by the pairing plus quadrupole model, but they did not calcualte the overall strength function or consider nuclei as large as ^{145}Gd.

The strength function S(E) of the external field $\hat{F}$ is defined by sum of overlaps between all the excited states $|f\rangle$ and the initial state $|0\rangle$. The expression of S(E) in the coordinate space using the particle-hole Green's function is derived in Ref. 1 which is given as

$$S(E) = \sum_f |\langle f|\hat{F}|0\rangle|^2 \delta(E_f - E_o - E) = \frac{1}{\pi}\int d^3r d^3r' F^*(r)\,\mathrm{Im}(G(r,r',E))F(r') \quad (1)$$

where G(r,r',E) is the particle-hole Green's function. The transformation from the particle-hole representation to the quasiparticle representation is straightforward and can be found in many standard text books.[7] For beta decay of odd mass nuclei, we start from a one-quasiparticle ground state and the Gamow-Teller operator connects to one- and three-quasiparticle excitations. The quasiparticle configurations of these states are depicted sybolically in Fig. 1 where (a) shows ground states of parent and daughter nuclei in β^+ decay and (b) shows one- and three-quasiparticle excitations with the excitation energy E_x in the daughter nucleus. The unperturbed Green's function

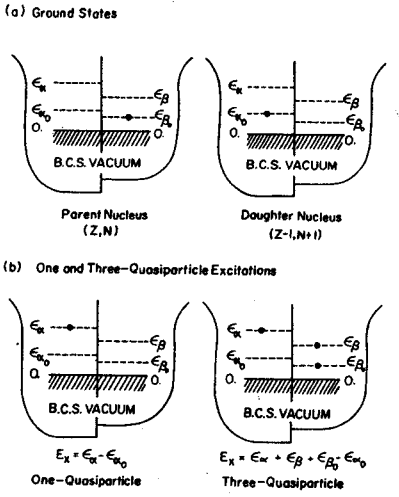

Fig. 1. Quasiparticle representation of ground states and excitations in β^+ decay of odd mass nuclei.

$G^o(E)$ for β^+ decays is thus given by two parts, one from one-quasiparticle and the other from three-quasiparticle excitations and can be written as:

$$G^o(E) = \sum_{\alpha}^{\text{single}} \frac{|\langle\alpha|\hat{F}|\beta_o\rangle|^2 v_\alpha^2 v_{\beta_o}^2}{\epsilon_\alpha - \epsilon_{\beta_o} - E} + \sum_{\alpha\beta}^{\text{Three}} \frac{|\langle\alpha\beta\beta|\hat{F}|\beta_o\rangle|^2}{\epsilon_\alpha + \epsilon_\beta - E} v_\alpha^2 U_\beta^2 \quad (2)$$

where α and β label quasiparticle states, U, V and ϵ the standard BCS amplitudes and energies and $|\beta_o\rangle$ the one-quasiparticle ground state of the parent nucleus. For Gamow-Teller decays, the operator F is given by

$$F = \sigma t_{\pm} \quad (3)$$

Thus the only difference between the theory of Ref. 2 and the present is the replacement of the particle-hole Green's function by Eq. 2.

In the pairing scheme, the basis of the response consists of two-quasiparticle states. Since much of the excitation energy comes from those energies, the result is quite sensitive to the spacing of the single particle spectrum. For that reason, we adjusted the spin-orbit strength of the single particle Hamiltonian to reproduce the known splitting of 0.75 MeV between $vs_{1/2}$ and $vh_{11/2}$ levels in ^{145}Gd. The pairing strength was adjusted to reproduce the empirical one quasiparticel energies of 0.88 and 0.95 MeV for neutrons and protons respectively. We determined for neutrons from the binding energy systematics of N=80, 81 and 82 and for protons from Z=62, 63 and 64 binding systematics.

In Table 1, we list low-lying excitations in ^{145}Eu which contribute to the Gamow-Teller strength function. The first column shows configurations of one- and three-quasiparticle states,

Table 1. Quasiparticle configurations

Configuration	E_x		VU or VV*	
	HF	WS	HF	WS
$(\pi s_{1/2})$	1.18	1.73	.19*	.16*
$(\pi d_{5/2}{}^{\nu}d_{3/2}{}^{\nu}s_{1/2})$	1.81	1.79	.35	.30
$(\pi h_{11/2}{}^{\nu}h_{11/2}{}^{\nu}s_{1/2})$	2.50	2.50	.12	.13
$(\pi d_{3/2}{}^{\nu}d_{3/2}{}^{\nu}s_{1/2})$	3.32	2.83	.08	.10
$(\pi d_{5/2}{}^{\nu}d_{5/2}{}^{\nu}s_{1/2})$	4.27	3.81	.09	.08
$(\pi d_{3/2}{}^{\nu}d_{5/2}{}^{\nu}s_{1/2})$	5.77	4.86	.02	.03
$(\pi g_{7/2}{}^{\nu}g_{7/2}{}^{\nu}s_{1/2})$	5.83	3.56	.08	.18
$(\pi h_{11/2}{}^{\nu}h_{9/2}{}^{\nu}s_{1/2})$	7.99	7.83	.45	.53
$(\pi g_{9/2}{}^{\nu}g_{7/2}{}^{\nu}s_{1/2})$	8.50	11.92	.18	.09

the second column the energy with respect to the ground state of ^{145}Eu. The last column gives the product of pairing amplitudes VU or V^2 for the three- or one- quasiparticle excitations respectively. The major low-lying peaks of Eq. 1 is tabulated in Table 2 together with the data of Ref. 5. The strengths S(E) are converted to the corresponding ft values by making use of the formula[8] for the Gamow-Teller decay given as

$$ft = 4140 \text{ sec}/S(E) \qquad (4)$$

The strength is normalized to 3 for the decay of an isolated proton. The first column is excitation energies with their unperturbed quasiparticle configurations. The second column is the log(ft) values. Although the calculated strength function reproduces the locations of the major peaks below 3 MeV excitation energy, we need an uniform quenching factor of about 40 to get the measured strengths. We show the log(ft) values after introducing this quenching factor inside the parentheses of the second column. The Hartree-Fock calculation shows the lowest peak at 1.3 MeV whereas Woods-Saxon does not have one. This is because of the difference in the single particle spectra between two models. In Woods-Saxon potential, the states $(\pi s_{1/2})$ and $(\pi d_{5/2}{}^{\nu}d_{3/2}{}^{\nu}s_{1/2})$ are nearly degenerate and give a single peak at 1.9 MeV. Our calculation also has some small peaks between major peaks which are not shown in Table 2. However, the theory does not have any state that corresponding to the measured 4.50 MeV peak though it shows a very strong state above 8.0 MeV, which is well outside the Q_+ window. The state has a structure $(\pi h_{11/2}{}^{\nu}h_{9/2}{}^{\nu}s_{1/2})$, which Firestone et al. identified with the observed 4.50 MeV peak. They argued that the spin-orbit energy was 5.5 MeV, and the residual interactin would lower this to 4.5 MeV. We have a much larger spin-orbit splitting, which is necessary to fit the neutron single particle

Table 2. Peaks of Gamow-Teller decay strength in ^{145}Gd.

Hartree-Fock		Woods-Saxon		Experiment	
E_x(MeV)	log(ft)(*)	E_x (MeV)	log(ft)(*)	E_x (MeV)	log(ft)
$1.3(\pi s_{1/2})$	4.4 (6.0)	-	-	1.04	6.5
$2.0(\pi d_{5/2}{}^{\nu}d_{3/2}{}^{\nu}s_{1/2})$	3.7 (5.3)	$1.9(\pi d_{5/2}{}^{\nu}d_{3/2}{}^{\nu}s_{1/2}) + (\pi s_{1/2})$	3.8 (5.4)	1.82	5.3
$2.5(\pi h_{11/2}{}^{\nu}h_{11/2}{}^{\nu}s_{1/2})$	4.3 (5.8)	$2.5(\pi h_{11/2}{}^{\nu}h_{11/2}{}^{\nu}s_{1/2})$	4.3 (5.9)	2.48	6.0
-	-	-	-	4.50	4.8
$8.5(\pi h_{11/2}{}^{\nu}h_{9/2}{}^{\nu}s_{1/2})$	3.1 (4.7)	$8.4(\pi h_{11/2}{}^{\nu}h_{9/2}{}^{\nu}s_{1/2})$	3.4 (5.0)	-	-

*log(ft) after quenching is introduced to the strength.

energies near the Fermi surface. Also the residual interaction in our model is repulsive and pushes the state up.

In conclusion, the nuclear response method of Ref. 1 is applied to the β^+ decay of ^{145}Gd with good agreement for the location of the lower states. However, our model can not account for the 4.50 MeV state. Also it gives the strength which is almost 10 times too large even after considering the well known quenching of the Gamow-Teller operators by factors 3-4.[9] One reason can be that the response method includes only the particle-hole interaction. The 4.50 MeV configuration resembles more a two-particle state, which has the opposite sign to the particle-hole interaction. Another possible reason is that we neglected the ground state correlations between neutrons and protons by using TDA. This may have considerable effect on the strength since the forward reaction is highly forbidden as discussed before. We are now extending the theory to include the particle-particle interaction as well as the RPA and we expect that this will lessen the disagreements for the overall strength and the energy of the highest strong state.

---

1. G.F. Bertsch and S.F. Tsai, Phys. Rep. 18 (1975) 125.
2. G.F. Bertsch, D. Cha and H. Toki, Phys. Rev. C24 (1981) 533.
3. K. Takahashi and M. Yamada, Progr. Theor. Phys. 41 (1969) 1470.
4. H.V. Klapdor and C.O. Wene, J. Phys. G6 (1980) 1061.
5. R.B. Firestone et al., to be published in Phys. Rev. C.
6. J.A. Halbleib, Sr. and R.A. sorensen, Nucl. Phys. A98 (1967) 542.
7. A.L. Fetter and J.D. Walecka, Quantum Theory of Many Particle Systems, McGraw-Hill, 1971.
8. A. Bohr and B.R. MOttelson, Nuclear Structure Vol. 1., W.A. Benjamin, 1969.
9. H. Ejiri and J.I. Fujita, Phys. Rep. 38 (1978) 86.

Giant M1 States in Zr Isotopes Within the Simple Shell Model

H. Toki, D. Cha and G. Bertsch

Very recently Anantaraman et al. have performed a (p,p') experiment at E_p = 200 MeV on the Zr isotopes and found for the first time giant M1 states in these nuclei.[1] The facts that M1 states are not found in ^{208}Pb and the above experimental findings in Zr isotopes motivated us to analyse the data with the simplest possible shell model.[2]

We assume that $og_{9/2}$ orbit is completely occupied by neutrons in ^{90}Zr and $ld_{5/2}$ orbit is started to be filled by increasing the neutron nubmer. The particle-hole interaction is further taken to be zero-range. The calculated results are compared with experiment in Table I. The experimental excitation energies are reproduced with $\bar{V}_\sigma$ = 370 MeV fm^3. This value indicates $V_\sigma \simeq V_{\sigma\tau}$. The calculated cross section shows a slight increase with mass number due to the $d_{3/2} - d_{5/2}^{-1}$ admixture and there seems to be a slight indication of this in the experiment. The calculated cross section, whose absolute value is obtained with reasonable assumptions on the interaction strength and the distortions, seems to need a factor of 2 quenching effect. This value is reasonalbe as the quenching factor for the magnetic strength in these nuclei.[3]

The newly observed M1 states are readily reproduced in terms of the simple shell model. The strength of the residual interaction and the quenching factor are both reasonable. Our present study may suggest that in fact M1 states with large M1 strength do exist in ^{208}Pb but so far they have not been detected due to the high level density.

1. N. Anantaraman et al., Phys. Rev. Lett. 46 (1981) 1318.
2. H. Toki, D. Cha and G. Bertsch, Phys. Rev. (1981).
3. H. Toki and W. Weise, Phys. Lett. 97B (1980) 12.

Table I. Experimental and calculated results for the excitation energies and the cross sections at θ = 4°. Calculated results with and without the residual interaction, $\bar{V}_\sigma$ = 370 MeV fm^3 and $\bar{V}_\sigma$ = 0 MeV fm^3 respectively, are shown in the second and the third columns.

	Exp		$\bar{V}_\sigma$ = 370 MeV fm^3		$\bar{V}$ = 0 MeV fm^3	
	E_x(MeV)	$\frac{d\sigma}{d\Omega}$(mb/sr)	E_x(MeV)	$\frac{d\sigma}{d\Omega}$(mb/sr)	E_x(MeV)	$\frac{d\sigma}{d\Omega}$(mb/sr)
^{90}Zr	8.90±0.15	2.8±0.3	8.9	5.9	6.2	5.9
^{92}Zr	8.8 ±0.2	2.8±0.3	8.9	6.3	6.2	5.9
			2.6	0.6	2.1	1.0
^{94}Zr	8.63±0.15	3.1±0.3	8.9	6.7	6.2	5.9
			3.1	1.1	2.1	2.0
^{96}Zr			8.9	7.2	6.1	5.9
			3.5	1.5	2.2	3.0

Systematics of the $\sigma\tau$ Strength in Nuclei

G. Bertsch, D. Cha and H. Toki

The recent studies with the (p,n) reaction at intermediate energies found systematically Gamow-Teller states for nuclei $A \geq 48$.[1] We tried to correlate the new data with a simple theoretical model.[2] Our model is based on the TDA and the RPA using either Woods-Saxon or Skyrme Hartree-Fock wave functions. We use a δ-function interaction and adjust the interaction strength so as to reproduce the main peak of the $\sigma\tau$ strength function. We apply also our model to the L=1 strength function.

We show in Table I the calculated results for the Gamow-Teller states ($J = 1^+$) for several nuclei. The use of the interaction strength $V_{\sigma\tau}$ = 220 MeV fm^3 with the Woods-Saxon wave functions enables us to reproduce the excitation energies within about 1 MeV. We obtain similar results with the Skyrme Hartree-Fock wave functions. Concerning the M1 strength, most of the strength is in the state at high excitation but there remains 20% of the total strength at low excitation, which is in agreement with the experimental findings in ^{48}Ca and ^{90}Zr.

We consider the L=1 strength associated with the spin flip process, because the $\sigma\tau$ interaction is dominant in the (p,n) reaction at high energies. Then we have the total spin states of J=0, 1 and 2. Our calculations show that the J=0 state is highest in energy. While nearly all of the strength is concentrated in a single state for J=0 and 1, the strength is spread over several states for J=2. We propose a possible spin-experiment to resolve the total spin J.

From this analysis, we extracted the interaction strength of $V_{\sigma\tau}$ = 200 MeV fm^3. This value corresponds to the Landau parameter of g' = 0.56. If the one-pion exchange is considered, the estimated g' would be of the order of 0.6, which is consistent with the general belief for this parameter.

Table I

Nucleus	Highest j	$\varepsilon(jj^{-1})$	$\varepsilon_{j_<} - \varepsilon_{j_>}$	E	E_{exp}
^{48}Ca	$f_{7/2}$	-0.2	6.0	10.3	10.4
^{90}Zr	$g_{9/2}$	-0.1	6.2	9.7	8.7
^{96}Zr	$g_{9/2}$	5.1	6.1	15.1	13.7
^{112}Sn	$g_{9/2}$	0.6	5.9	9.7	9.5
^{114}Sn	$h_{11/2}$	2.9	6.6	14.1	13.9
^{169}Tm	$h_{11/2}$	6.2	6.2	16.5	15.5
^{208}Pb	$i_{13/2}$	3.6	6.6	14.7	15.5

Table I. Gamow-Teller energies. $\varepsilon(jj^{-1})$ denotes the excitation energy of the $j_> - j_>^{-1}$ state and $\varepsilon_{j_<} - \varepsilon_{j_>}$ the spin-orbit splitting. The diagonalized energy E is compared with the experimental value E_{exp}.

1. D.E. Bainum et al., Phys. Rev. Lett. 44 (1980) 1751; B.D. Anderson, et al., Phys. Rev. Lett. 45, (1980) 699; D.J. Horen, et al., Phys. Lett. 95B (1980) 27.
2. G. Bertsch, D. Cha and H. Toki, Phys. Rev. C24 (1981) 533.

Proximity to the rho Meson Condensation Threshold in Nuclei

H. Toki and J.R. Comfort[+]

Motivated by the sensitivity of the magnetic form factor at large momentum (the operator has the form $\vec{\sigma}\times\vec{q}$) to the rho meson interaction strength, we made a systematic study of the critical threshold to the spin-isospin instability driven by either or both of the $\vec{\sigma}\times\vec{p}$ and $\vec{\sigma}\cdot\vec{q}$ correlations in nuclei.[1] The particle-hole interaction has the form[2]

$$W_{ph}(q) = (V_\pi(q)\vec{\sigma}_1\cdot\hat{q}\vec{\sigma}_2\cdot\hat{q} + V_{2\pi}(q)\vec{\sigma}_1\times\hat{q}\vec{\sigma}_2\times\hat{q} + g'(q)\vec{\sigma}_1\cdot\vec{\sigma}_2 + h'(q)S_{12}(q))\vec{\tau}_1\cdot\vec{\tau}_2$$

where the first and the second terms are the one pion (OPE) and two pion exchanges (TPE) in the isovector channel, respectively. All the remaining many-body correlations are introduced in the phenomenological Landau short-range interaction g' and the tensor interaction h'. While g' is believed to range between 0.5 and 0.7 in the units of f_π^2/m_π^2 at q = 0, h' is negligibly small.

This interaction is treated within the random phase approximation and the appearence of the zero energy solution of the RPA equation is used for determination of the critical threshold.[3] For example, we show in Fig. 1 the calculated results for the critical g' at and below which the spin-isospin instability is realized as a function of the strength of the $\vec{\sigma}\times\hat{q}$ correlation C_ρ.

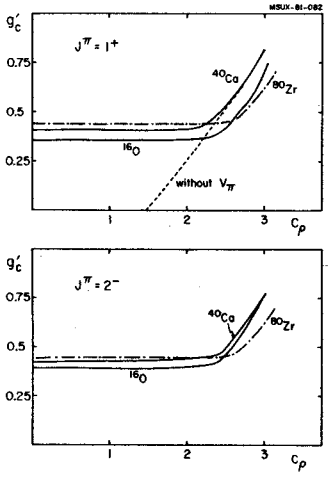

Fig. 1. The critical value g' for $J^\pi = 1^+$ and 2^- states in ^{16}O, ^{40}Ca and ^{90}Zr as a function of the rho mesion coupling strength C_ρ. The dashed curve is obtained with $V_\pi = 0$ for ^{40}Ca.

One sees that g'_c is nearly constant up to $C_\rho \sim 2.2$-2.5 for different nuclei and then rises rapidly after that. To elucidate the behavior, calculations are also done for the 1^+ state of ^{40}Ca with $V_\pi = 0$ and the results are shown as the dashed line in Fig. 1. This behavior of g'_c suggests the interesting fact that the $\vec{\sigma}\cdot\hat{q}$ correlation caused by V_π and the $\vec{\sigma}\times\hat{q}$ correlation of $V_{2\pi}$ neither interfere nor cooperate very much in bringing about the nuclear instability, even in nuclei as small as ^{16}O. Thus, one can talk the pion instability and rho meson instability separately in nuclei.

Since the full two pion exchange strength as determined from empirical NN→2π data,[4] corresponds to $C_\rho \sim 2.8$, although this value might be somewhat reduced by the Pauli blocking, the results suggest that the nuclear phase transition is closer to the rho mesonic instability than to the pionic instability. A further implication of this would be that precritical phenomena would be more pronounced in processes dominated by the $\vec{\sigma}\times\hat{q}$ interaction such as (e,e') reaction than in the processes caused by the $\vec{\sigma}\cdot\hat{q}$ interaction such as (p,p'), (π,γ) reactions.

Because while our discussions depend on the size of the $\vec{\sigma}\times\hat{q}$ correlation strength in nuclei, which is less explored, we need to make systematic experimental studies on the high momentum properties of nuclei in all mass regions.

+ Department of Physics and Astronomy, University of Pittsburgh, Pittsburgh, Pennsylvania 15260.

1. H. Toki and J.R. Comfort, preprint (1981), Michigan State University.
2. H. Toki and W. Weise, Phys. Rev. Lett. 42 (1979) 1034.
3. H. Toki and W. Weise, Z. Phys. A292 (1979) 389.
4. G. Hohler and E. Pietarinen, Nucl. Phys. B95 (1979) 210 and a recent publication from Univ. of Karsruhe.